Advances in Medical Sciences 69 (2024) 434–442

Contents lists available at ScienceDirect

Advances in Medical Sciences

journal homepage: www.elsevier.com/locate/advms

Original research article

Differentiation of solid and friable tumour thrombus in patients with renal cell carcinoma: The role of MRI apparent diffusion coefficient

Paweł Kowal [a,*], Krzysztof Ratajczyk [a], Wiktor Bursiewicz [a], Maciej Trzciniecki [a], Karolina Marek-Bukowiec [b], Joanna Rogala [c], Vasyl Kowalskyi [d], Jozef Dragasek [e], Andrea Botikova [f], Peter Kruzliak [g,**], Yulian Mytsyk [h]

[a] Department of Urology, Regional Specialist Hospital, Wroclaw, Poland
[b] Research and Development Center, Regional Specialist Hospital, Wroclaw, Poland
[c] Department of Pathology, Regional Specialist Hospital, Wroclaw, Poland
[d] Department of Oncology and Radiology, Danylo Halytsky Lviv National Medical University, Lviv, Ukraine
[e] Faculty of Medicine, Pavol Jozef Safarik University and University Hospital, Kosice, Slovakia
[f] Faculty of Health and Social Work, Trnava University, Trnava, Slovakia
[g] 2nd Department of Surgery, Faculty of Medicine, Masaryk University and St. Anne's University Hospital, Brno, Czech Republic
[h] Department of Urology, Danylo Halytsky Lviv National Medical University, Lviv, Ukraine

ARTICLE INFO

Keywords:
Renal cell carcinoma
Thrombus
Diffusion-weighted imaging
Texture analysis

ABSTRACT

Purpose: Inferior vena cava (IVC) involvement by renal cell carcinoma (RCC) is associated with a higher disease stage and is considered a risk factor for poor prognosis. This study aimed to investigate the role of the apparent diffusion coefficient (ADC) of MRI 3D texture analysis in the differentiation of solid and friable tumour thrombus in patients with RCC.

Materials and methods: The study involved 27 patients with RCC with tumour thrombus in the renal vein or IVC, surgically treated with nephrectomy and thrombectomy and in whom preoperatively abdominal MRI including the DWI sequence was conducted. For 3D texture analysis, the ADC map was used, and the first-order radiomic features were calculated from the whole volume of the thrombus. All tumour thrombi were histologically classified as solid or friable.

Results: The solid and friable thrombus was detected in 51.9 % and 48.1 % of patients, respectively. No differences in mean values of range, 90th percentile, interquartile range, kurtosis, uniformity and variance were found between groups. Equal sensitivity and specificity (93 % and 69 %, respectively) of ADC mean, median and entropy in differentiation between solid and friable tumour thrombus, with the highest AUC for entropy (0.808), were observed. Applying the skewness threshold value of 0.09 allowed us to achieve a sensitivity of 86 % and a specificity of 92 %.

Conclusions: In patients with RCC and tumour thrombus in the renal vein or IVC, the 3D texture analysis based on ADC-map allows for precise differentiation of a solid from a friable thrombus.

1. Introduction

The global incidence of kidney cancer is estimated at approximately 431,288 new cases, with 138,611 occurring in Europe. The majority of these cases, around 90 %, are attributed to renal cell carcinoma (RCC) [1]. The high mortality rate of this disease prompts the research for novel radiological and molecular biomarkers for early diagnosis. Within this context, exosomes have emerged as a novel source of non-invasive molecular tumour biomarkers. The unique bilayer membrane structure of exosomes offers protection against external RNases and proteases, leading to enhanced stability of the enclosed mRNAs, miRNAs, and functional proteins, thus making exosomes highly sensitive markers for disease diagnosis. The cargo in tumour-derived exosomes, such as the range of miRNAs, can also serve as biomarkers for clear cell RCC in patients' serum

* Corresponding author. Department of Urology, Regional Specialist Hospital, Kamieńskiego 73a, 51Wroclaw, Poland.
** Corresponding author. 2nd Department of Surgery, Faculty of Medicine, Masaryk University and St. Anne's University Hospital, Pekařská 53, 656 91, Brno, Czech Republic.
E-mail addresses: pawelkowal13@gmail.com (P. Kowal), kruzliakpeter@gmail.com (P. Kruzliak).

https://doi.org/10.1016/j.advms.2024.09.002
Received 17 January 2024; Received in revised form 12 March 2024; Accepted 13 September 2024
Available online 14 September 2024

and urine, offering valuable targets for early detection and monitoring of the disease [2,3].

On the other hand, recent research emphasizes the vital importance of magnetic resonance imaging (MRI) markers like the apparent diffusion coefficient (ADC) in detecting kidney cancer despite their current omission from routine clinical usage [4]. Statistical models indicate that age-adjusted rates for new kidney cancer cases have risen by an average of 0.6 % annually over the past 5 years [5]. In recent findings, new favourable subsets of cancers of undefined origin are emerging, resembling RCC, suggesting a correlation with the current rise in this disease incidence [6]. This data underscores the significance of discovering precise preoperative biomarkers for kidney cancer.

RCC is well known for its propensity for extension into the inferior vena cava (IVC), which accounts for 4–10 % of all RCC cases [7]. Extension of the tumour into the IVC is associated with a higher disease stage and is considered a risk factor for recurrence and poor prognosis [8]. To date, an aggressive surgical approach is the gold standard in the management of most patients with IVC thrombus, offering the only chance of long-term survival [9,10]. As RCC extending to IVC may pose severe complications during the operation, the surgical approach to meta thrombus plays a tremendous role in treatment outcome. The tumour volume is one of the primary but not the only factor impacting the choice of surgical approach, surgical complexity and postoperative complications [11]. Thrombi macroscopically described as solid, with regular surfaces, are easier to manage than irregular, friable surfaces with a high probability of crashing into smaller pieces, resulting in thrombo-embolic and potentially fatal complications [12]. It has been proven that the presence of a friable thrombus in IVC increases the difficulty of surgery and is associated with adverse survival outcomes in patients with RCC; the presence of a friable thrombus was associated with statistically significantly lower median cancer-specific survival compared to the solid variant (28 vs 76 months, respectably; $P < 0.001$) [13–16]. An accurate prediction of thrombus consistency type in presurgical imaging studies may help to better design the surgical procedures and avoid pulmonary embolism during nephrectomy or thrombectomy [17]. However, preoperative differential diagnostics of tumour thrombus consistency on imaging is still challenging and friable thrombus can be misdiagnosed as bland [18,19]. There is a paucity of scientific data on this topic. Several imaging modalities, such as preoperative contrast-enhanced computed tomography (CT) and intraoperative contrast-enhanced ultrasound (CEUS), were recently investigated to define the accurate techniques feasible for differentiating solid and friable IVC thrombus; however, none was widely accepted [20–22]. Earlier, it was demonstrated that qualitative analysis of diffusion-weighted imaging (DWI) and ADC of MRI allowed for accurate differentiation of solid from bland thrombus of the portal vein in patients with hepatocellular carcinoma (HCC) [23]. Nevertheless, such results appeared to be conflicting [24]. The diagnostic performance of MR-DWI in distinguishing bland from friable thrombus in IVC of patients with RCC still needs to be comprehensively assessed. This study aimed to investigate the role of ADC of MRI 3D texture analysis in the differentiation of solid and friable tumour thrombus in patients with RCC.

2. Materials and methods

2.1. Patients

This retrospective study, conducted between 2022 and 2023, utilized clinical and radiological data collected from 2011 to 2023 from the database of the Department of Urology at the Regional Specialist Hospital in Wroclaw. Initially, a cohort of 69 patients diagnosed with RCC and tumour extension into the IVC was enrolled. The inclusion criteria were patients with pathologically confirmed RCC with the spread of the tumour thrombus into the renal vein or IVC, surgically treated with nephrectomy accompanied by thrombectomy and in whom preoperative abdominal MRI including the DWI sequence as an integral part was conducted. The exclusion criteria for this study included the lack of the ADC map in the MRI data and the absence of histological verification of the diagnosis. Therefore, 27 cases were selected for further analysis: 14 males and 13 females. The mean age of patients was 62.81 ± 6.69 years (range, 47–74 years). Based on the histological report, all patients were stratified into one of the two groups depending on the consistency of the thrombus - solid or friable (Table 1).

2.2. Histological examination

Thrombi were sent for histological examination either removed *en bloc* with the kidney or as separate pieces of tissue. Thrombi forming solid mass were cut longitudinally, with a representative whole cross-section of the thrombus submitted for histology, while pieces of friable thrombi were submitted randomly. Standard pathologic criteria for submitting material were applied to make it the best representative: one section per one cm of the thrombus length. On macroscopic examination, thrombi presented as cohesive masses with regular outlines or as fragile pieces of tissue. The microscopic examination was focused on estimating the percentage of viable tumour cells in each thrombus. It ranged from 0 % (no cells) to 90 % of the thrombus surface. The histological composition of the thrombus was deemed solid if it comprised more than 50 % of tumour cells and exhibited solid attributes characterized by density, coherence, a rounded linear profile, and an endothelial lining resembling a pseudo capsule. The non-cellular surface of the friable thrombi was occupied mainly by fibrin, haemorrhages or non-viable, necrotic tumour cells (Fig. 1). In addition, in all cases, during the nephrectomy/thrombectomy, the same surgeon assessed the concordance between the surgical and pathological consistency.

2.3. MRI technique

MRI was performed using a 1.5 T body scanner (Signa HDxt, General Electric, Wisconsin, USA) using an 8-channel phased-array body coil. The MRI protocol included sequences with the following parameters: coronal T2-weighted single-shot fast spin-echo (SSFSE), repetition time (TR) = 2625 ms, echo time (TE) = 90 ms, flip angle = 90°, field of view (FOV) =

Table 1
Patient characteristics and descriptive statistics.

Variable	All patients (n = 27)	Solid VTT (n = 14)	Friable VTT (n = 13)	*p*-value
Age, years				0.712*
Mean (median)	62.81 (65.0)	63.29 (65.0)	62.31 (62.0)	
Range	47–74	47–74	49–74	
Sex, n (%)				0.842§
Male	14 (51.9)	7 (25.9)	7 (25.9)	
Female	13 (48.1)	7 (25.9)	6 (22.2)	
Tumour side, n (%)				0.816§
Right	16 (59.3)	8 (29.6)	8 (29.6)	
Left	11 (40.7)	6 (22.2)	5 (18.5)	
T-stage, n (%)				0.964§
T3a	9 (33.3)	5 (18.5)	4 (14.8)	
T3b	12 (44.4)	6 (22.2)	6 (22.2)	
T3c	6 (22.2)	3 (11.1)	3 (11.1)	
N-stage, n (%)				0.936§
N0	23 (85.2)	12 (44.4)	11 (40.7)	
N1	4 (14.8)	2 (7.4)	2 (7.4)	
M-stage, n (%)				0.936§
M0	23 (85.2)	12 (44.4)	11 (40.7)	
M1	4 (14.8)	2 (7.4)	2 (7.4)	
Tumour grade				0.989§
Grade 2	6 (22.2)	3 (11.1)	3 (11.1)	
Grade 3	17 (63.0)	9 (33.3)	8 (29.6)	
Grade 4	4 (14.8)	2 (7.4)	2 (7.4)	

Abbreviations: VTT - venous tumour thrombus, SD – standard deviation, * - Student *t*-test, § - χ^2 test.

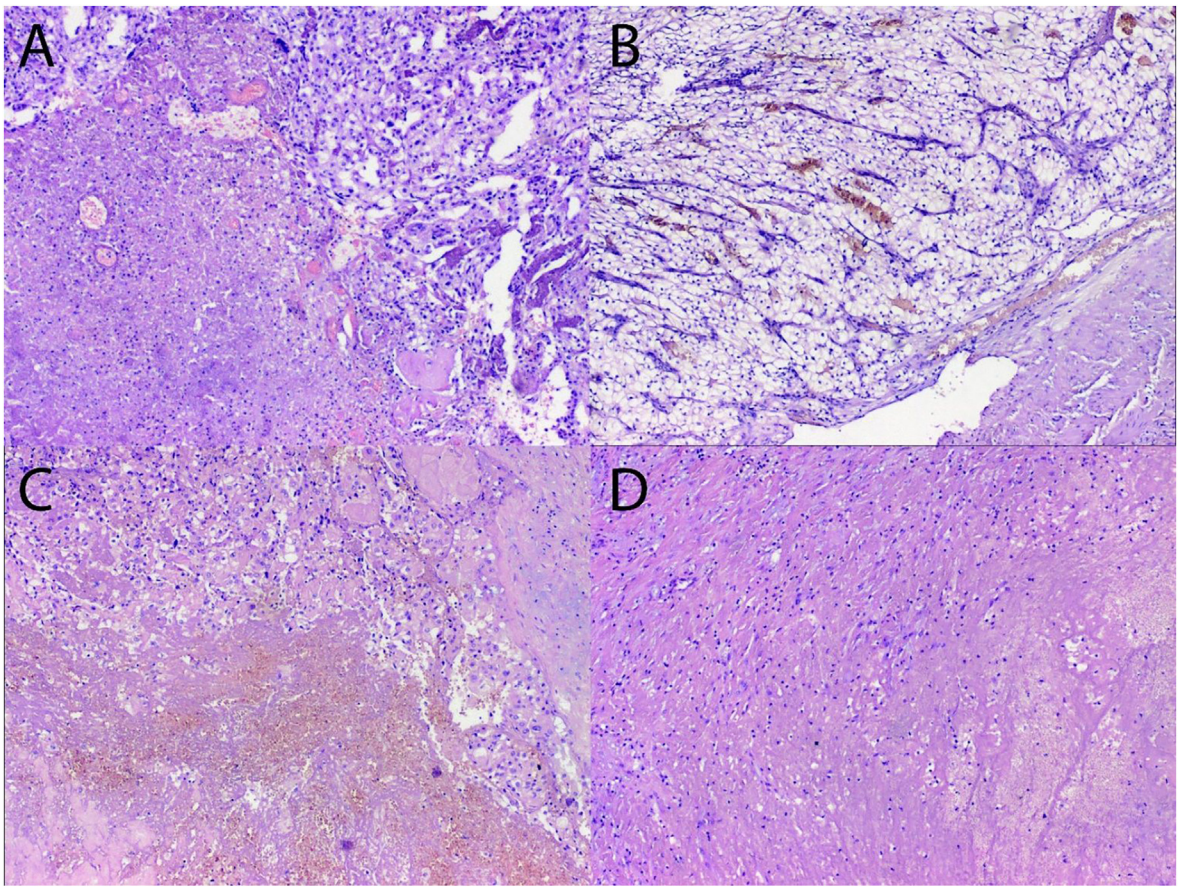

Fig. 1. Microphotography of the RCC tumour thrombus of solid and friable histologic consistency, hematoxylin and eosin, × 40. (A) A friable thrombus consistency, <50 % of tumour cells, necrotic tumour tissue in the lower left corner; (B) a solid thrombus consistency, tumour thrombus composed of 90 % of tumour cells, the lower left wall of IVC; (C) and (D) a friable thrombus consistency, <50 % of tumour cells, the regions of haemorrhages and fibrin are present.

40 × 40 cm, matrix = 200 × 192, breath-hold; axial 2D fast imaging employing steady-state acquisition with fat saturation (FIESTA FAT SAT), TR = 4.1 ms, TE = 1.8 ms, flip angle = 90°, FOV = 40 × 40 cm, matrix = 224 × 320; sagittal T2-weighted SSFSE, TR = 1760 ms, TE = 87.4 s, flip angle = 90°, FOV = 37 × 37 cm, matrix = 384 × 256; axial T1-weighted fast spoiled gradient-recalled echo dual-echo (FSPGR-DE), TR = 130 ms, TE = 2.1 ms and 4.3 ms, flip angle = 70°, FOV = 43 × 43 cm, matrix = 320 × 192, breath-hold; axial DWI, TR = 12000 ms, TE = 90 ms, FOV = 40 × 40 cm; matrix = 200 × 192; NEX = 3; bandwidth = 250 kHz, diffusion direction = slice, slice thickness = 6.0 mm, interscan gap = 1.0 mm with b-values = 50, 200, 800 s/mm^2, performed prior to contrast media administration, using single-shot echo-planar imaging sequence with parallel imaging technique and fat saturation during one breath-hold; axial 3D fat-saturated T1-weighted spoiled gradient echo liver acquisition with volume acquisition (LAVA), TR = 4.5 ms, TE = 2.2 ms, flip angle = 15°, FOV = 38 × 38 cm, matrix = 320 × 192, during, and following administration of gadolinium diethylenetriamine pentaacetic acid (Gd-DTPA) in a dose of 0.1 mmol/kg of body weight as a bolus injection with 20 s between each breath-hold acquisition.

2.4. 3D texture analysis

The MRI data interpretation was performed qualitatively by visually evaluating the T1-WI, T2-WI and DWI images and the corresponding ADC map. A colour ADC map was generated at the workstation (Advantage Windows, GE Healthcare, Wisconsin, USA); the Functool 4.5 software (https://www.functool.com) was used. The MRI images were evaluated by two experienced radiologists with 15 and 10 years of experience in kidney imaging. The image readings were performed by consensus. There was perfect interobserver agreement (kappa = 1.0). The 3D Slicer v.5.0.2 software (https://www.slicer.org) was used to extract the volumetric data and texture analysis. The region of interest (ROI) was placed over the region of the thrombus (including the renal vein), carefully repeating its contour on each slice directly on the ADC maps; this segmentation was used to generate a 3D model of the thrombus (Fig. 2). For the 3D texture analysis, the ADC map was used, and the following radiomic first-order features were calculated from the whole volume of the thrombus: ADC mean, median, range, 10th percentile, 90th percentile, interquartile range (IQR), entropy, kurtosis, skewness, uniformity and variance. Care was taken to avoid including the IVC wall in the ROI.

2.5. Statistical Analysis

SPSS Statistics for Windows, version 22.0 (IBM Corp., Armonk, NY, USA) was used for data processing. The radiomic features were expressed as mean ± standard deviation (SD). Differences among categoric variables were assessed utilizing the χ^2 test. The normality of the data was assessed using the Kolmogorov-Smirnov and the Shapiro-Wilk tests. Given the non-normality of the data distribution, the radiomic features in solid and friable thrombi cohorts were compared using the Mann-Whitney test. For the correlation analysis, the Pearson method was used. The diagnostic performance of radiomic features was measured using the receiver operating characteristics (ROC) analysis. The results were considered statistically significant when the p-value was <0.05.

2.6. Ethical issues

The study was approved by the Local Bioethical Committee at the

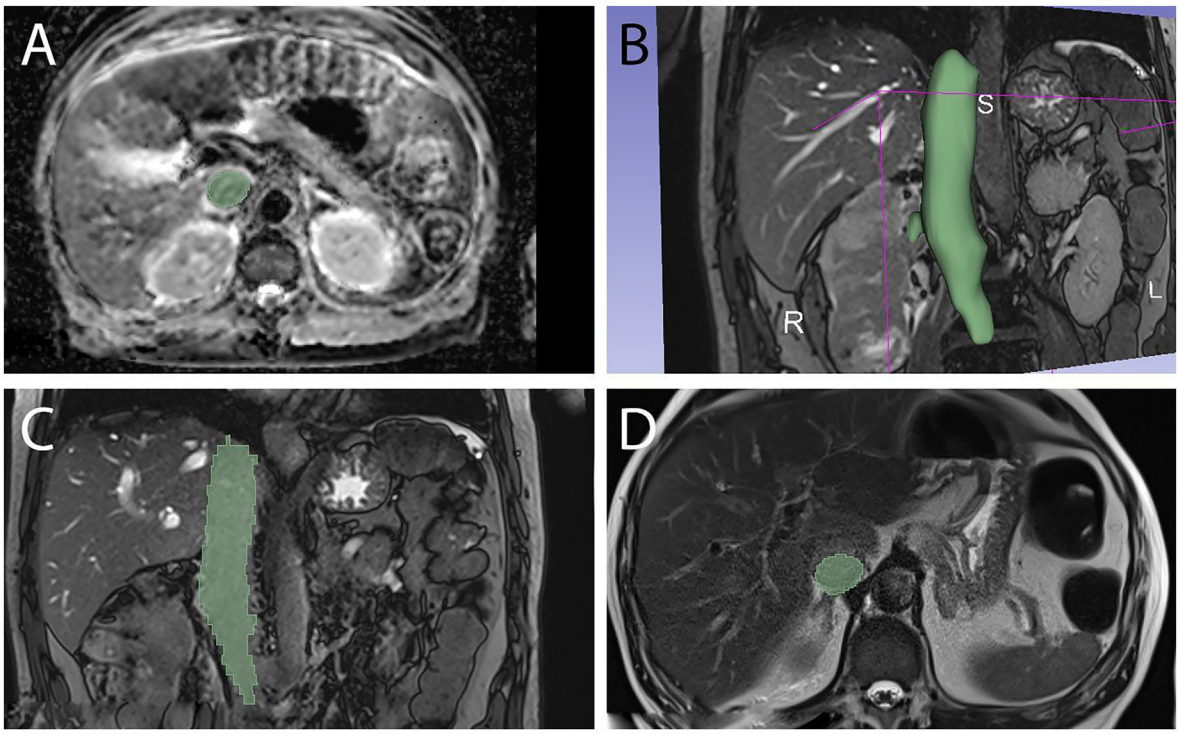

Fig. 2. Abdominal MRI of a 66 years old patient, with the right kidney conventional RCC and tumour thrombus in IVC, T3bN0M0, G3. (A) ADC map with region of interest (ROI) over the region of the tumour thrombus in IVC; (B) 3D model of the tumour thrombus processed from the segmentation of ADC map, thrombus volume = 77 cm^3; (C) and (D) T2-WI in coronal and axial projections with the corresponding ROIs.

Research and Development Center, Regional Specialist Hospital in Wroclaw, Poland (approval number: KB/12/2021). All procedures performed in studies followed the ethical standards of the institutional and national research committee and the 1964 Helsinki Declaration with its later amendments. All patients signed the written informed consent for enrolment in the study.

3. Results

In 16 cases (59.3 %), tumours were located in the right kidney, and in 11 cases (40.7 %) they were located in the left kidney. All patients were categorized according to the TNM classification: 9 (33.3 %) patients with T3a stage, 12 (44.4 %) patients with T3b stage and 6 (22.2 %) patients with T3c stage. The involvement of metastatic lymphatic nodules and the presence of distant metastasis was observed in 4 (14.8 %) cases. The distribution of the RCC grades was as follows: Grade 2–6 (22.2 %) patients, Grade 3–17 (63.0 %) patients, and Grade 4–4 (14.8 %) cases. According to histological examination, the solid thrombus was detected in 14 (51.9 %) patients, while the friable tumour variant was found in 13 (48.1 %) patients. The mean percentage of tumour cells within venous tumour thrombus (VTT) in groups with solid and friable variants was 69.29 ± 12.69 % and 32.31 ± 18.33 %, respectively ($p < 0.001$). In all cases, the histologic subtype of RCC was clear-cell. There was no difference in age, sex, tumour side, T-stage and grade in groups of patients with solid and friable thrombus. The mean volume of the thrombi also did not differ in both groups: 59.22 ± 48,39 cm^3 (range, 12.7–157.04 cm^3) in solid vs 60.44 ± 28.36 cm^3 (range, 23.56–112.34 cm^3) in friable tumour ($p > 0.05$).

The retrospective analysis uncovered perioperative complications in 5 (18.52 %) patients: thrombus detachment during thrombectomy occurred in 1 (3.7 %) case, while pulmonary embolisms were observed before and after surgical intervention in 2 (7.4 %) and 2 (7.4 %) patients respectively. In every instance, these complications were identified in patients with VTTs comprising less than 50 % of tumour cells (exclusively in friable VTTs, $p < 0.001$).

As a result of 3D texture analysis, no significant difference in mean values of such radiomic features as range, 90th percentile, IQR, kurtosis, uniformity and variance was found between the groups ($p > 0.05$). Nonetheless, a significant difference between the groups with solid and friable thrombus was detected in such texture parameters as mean ADC value, median, 10th percentile, entropy and skewness. The mean ADC value of the whole volume of the thrombus was statistically significantly higher in the group of patients with solid thrombi compared to those with the friable thrombi. It amounted to 1454.16 ± 243.93 vs 1219.45 ± 114.88 mm^2/s, respectively ($p = 0.002$). The mean 10th percentile value in solid compared to friable thrombi demonstrated a similar tendency and was 1091.36 ± 284.0 vs 885.67 ± 260.92 mm^2/s, respectively ($p = 0.039$). Likewise, the mean entropy value was statistically significantly higher in the group with solid thrombi compared to those with the friable thrombi: 5.69 ± 0.44 vs 5.27 ± 0.31, respectively ($p = 0.006$). Also, there was a difference in mean skewness values between solid and friable thrombus groups: −0.29 ± 0.47 vs 0.52 ± 0.42, respectively ($p < 0.001$) (Fig. 3). The detailed statistical characteristics of the radiomic features in both groups of patients are presented in Table 2.

We analyzed the associations between the percentage of RCC cells in tumour thrombus and the values of the radiomic features, which demonstrated a significant difference between groups of patients with diverse thrombus consistency, namely: mean ADC value, median, 10th percentile, entropy and skewness. According to correlation analysis, there was a strong direct association between the percentage of RCC cells in tumour thrombus and the mean ADC value, median, 10th percentile and entropy. However, the strongest was an inverse association between the percentage of RCC cells in tumour thrombus and skewness (Table 3; Fig. 4). There were no associations between the RCC grade and radiomic features of the thrombi ($p < 0.05$).

The ROC analysis demonstrated equal sensitivity and specificity (93 % and 69 %, respectively) of such radiomic features as ADC mean, median and entropy in differentiation between solid and friable tumour thrombus in patients with RCC, with the largest area under the curve (AUC) for entropy (AUC = 0.808; 95 % confidence interval [CI] =

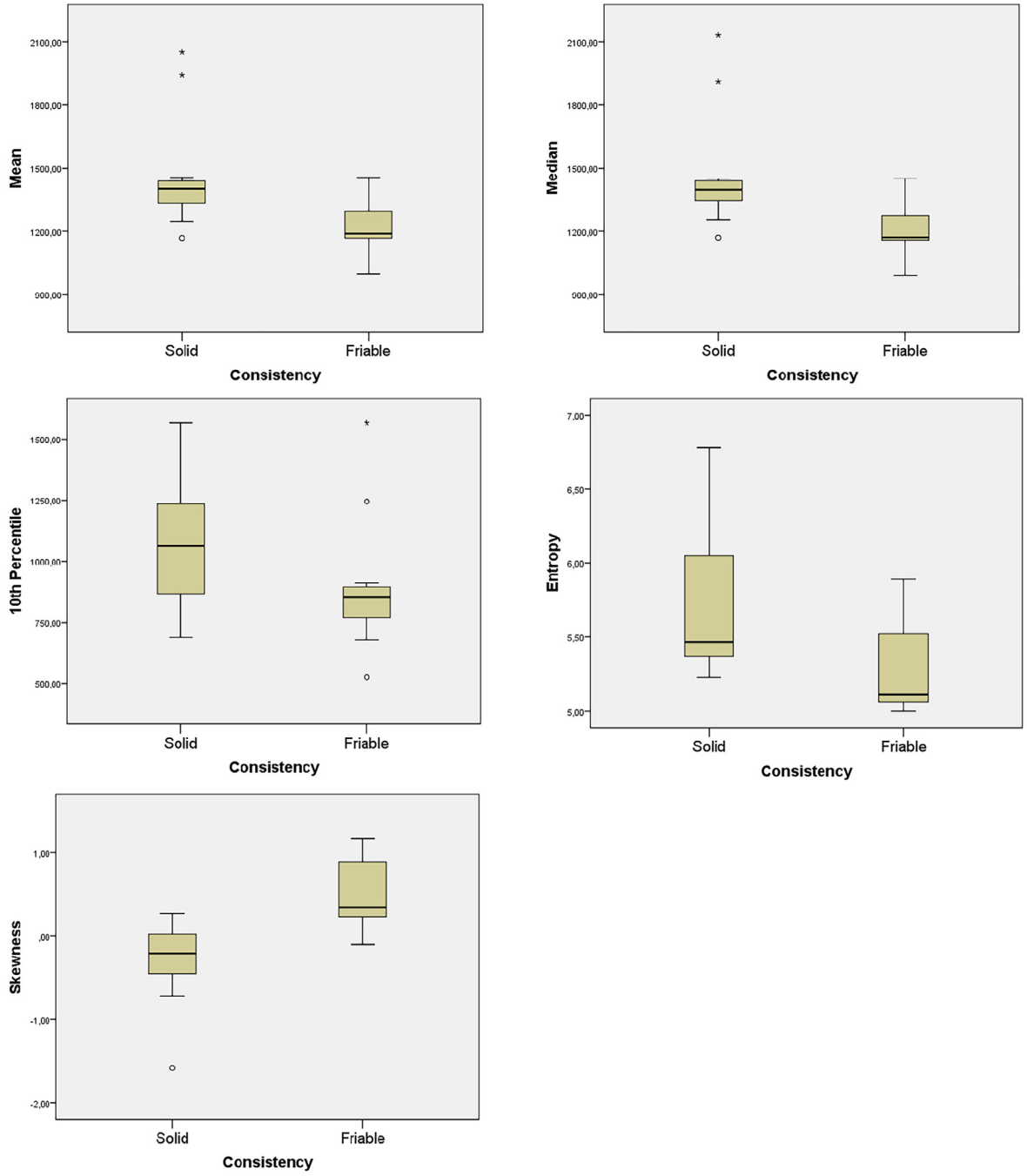

Fig. 3. Box plots of the mean ADC value, median, 10th percentile, entropy and skewness in groups of patients with RCC and with solid and friable thrombus consistency according to the 3D texture analysis.

0.633–0.983). At the same time, the application of the skewness threshold value of 0.09 allowed us to achieve a sensitivity of 86 % and specificity of 92 % with the highest performance of the model (AUC = 0.931; 95 % CI = 0.840–1.0) (Table 4; (Fig. 5A andB).

An intraoperative palpatory test revealed a complete concordance between the surgical and pathologic consistency in 100 % of cases (k = 1.0) (Fig. 6).

4. Discussion

The presence of friable venous tumour thrombus in patients with RCC significantly affects the prognosis: according to systematic review and meta-analysis by Qin et al. [25], the friable variant of thrombus in IVC was a predictor of poor overall survival using the fixed-effort model (pooled HR = 1.60; 95 % CI, 1.13–2.26). Nevertheless, this topic remains under active debate and is not devoid of controversy. Previously, it was believed that the consistency of the tumour thrombus in IVC of patients with RCC does not affect the choice of surgical tactics [26]. However, today approaches to this issue have changed. Accurate preoperative differentiation of friable from solid tumour thrombus in patients with RCC spread into IVC plays an essential role in surgical treatment planning [14,17]. Misdiagnosing the friable thrombus may lead to such fatal complications as pulmonary embolism [12]. Bertini et al. [27] documented that the consistency of VTTs could serve as an independent predictor of an unfavourable clinical trajectory. In particular, patients with VTT displaying fragile characteristics, such as irregular shape,

Table 2
The detailed statistical characteristics of the ADC map-based radiomic features in groups of patients with RCC and with solid and friable thrombus consistency according to the 3D texture analysis.

Radiomic feature	Solid thrombus (n = 14)			Friable thrombus (n = 13)			*p*-value
	Mean	SD	95 % CI	Mean	SD	95 % CI	
Mean, mm^2/sec	1454.16	243.93	1313.32–1595.0	1219.45	114.88	1150.02–1288.87	0.002
Median, mm^2/sec	1457.54	254.52	1310.58–1604.49	1211.77	115.61	1141.91–1281.63	0.001
Range, mm^2/sec	2576.29	278.11	2415.71–2736.86	2613.69	421.15	2359.20–2868.19	0.846
10th percentile, mm^2/sec	1091.36	284.0	927.38–1255.34	885.67	260.92	728.00–1043.34	0.039
90th percentile, mm^2/sec	1649.63	440.02	1395.57–1903.69	1516.72	85.31	1465.16–1568.27	0.645
IQR, mm^2/sec	433.57	93.13	379.80–487.34	407.02	59.90	370.82–443.22	0.752
Entropy	5.69	0.44	5.44-5.95	5.27	0.31	5.08-5.46	0.006
Kurtosis	4.26	1.16	3.59-4.93	3.89	1.11	3.22-4.56	0.331
Skewness	−0.29	0.47	−0.56–−0.02	0.52	0.42	0.27-0.78	<0.001
Uniformity	0.03	0.01	0.02-0.03	0.02	0.01	0.02-0.03	0.845
Variance	109747.60	72193.11	68064.54–151430.66	93341.99	28707.81	75994.04–110689.95	0.75

Abbreviations: SD – standard deviation, CI – confidence interval, IQR - interquartile range.

Table 3
Associations between the percentage of RCC cells in tumour thrombus and radiomic features.

Radiomic feature	Pearson correlation coefficient	P value
Mean	0.720	<0.001
Median	0.715	<0.001
10th percentile	0.635	<0.001
Entropy	0.713	<0.001
Skewness	−0.799	<0.001

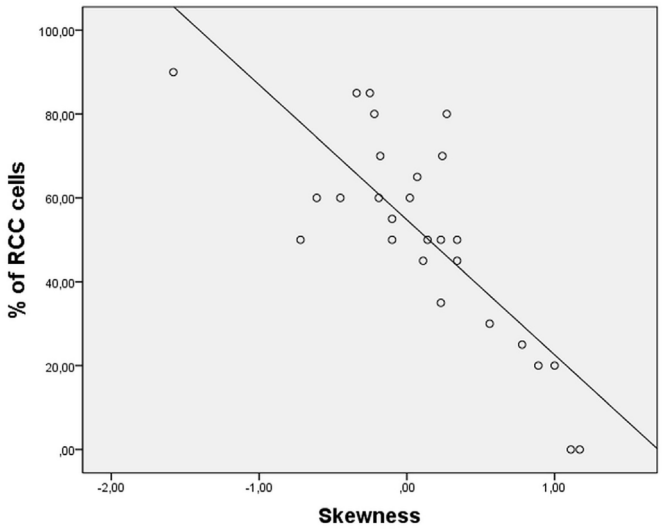

Fig. 4. The scatter plot of the association between the percentage of RCC cells in VTT and skewness.

fragmented appearance, necrosis, and fibrin exudate, experienced poorer outcomes. The results presented by Ayyathurai et al. [12] unmistakably suggest that a friable thrombus alongside the tumour thrombus should signal the surgical team to anticipate a potentially intricate and demanding surgical scenario. One out of two (50 %) patients with concomitant bland thrombus required surgical interruption of the IVC. Among patients with bland thrombus, 27 % underwent intraoperative IVC filter placement, and 80 % required at least one additional surgical procedure [12]. A heightened tumour thrombus level can induce greater resistance as blood flows back into the right atrium, leading to significantly abnormal hemodynamics and heightened potential for endothelial damage. This is corroborated by the findings of Wang et al. [28], who indicate that an elevated level of tumour thrombus ($p = 0.004$) and invasion of the IVC wall ($p = 0.030$) were significantly linked to the presence of friable VTT. As mentioned earlier, unlike solid tumour thrombus, which displays a unified and dense structure with an intact pseudo capsule, friable tumour thrombus exhibits an irregular, fragmented shape with numerous areas of necrosis, rendering them more susceptible to collapse and shedding. Consequently, friable VTTs could harbor shed tumour cells or tissue, potentially fostering tumour progression even after the complete removal of the tumour thrombus. This is especially pertinent for distant friable VTTs, considering the common practice of IVC interruption or ligation without removal of the friable thrombus [12,29]. In our study, we found that perioperative complications, including thrombus detachment during thrombectomy and pulmonary embolism before and after surgery, occurred in 18.52 % of cases. Notably, these complications were consistently found in patients with friable VTTs comprising less than 50 % tumour cells, characterized by a substantial amount of fibrin, haemorrhages, or non-viable necrotic tumour cells. Our data support the validity of using a threshold of more than 50 % tumour cells in the thrombus to define its solid consistency. Additionally, our findings suggest that the presence of a prominent fragile thrombus component, such as blood clots and fibrin, may contribute to embolism in fragile thrombus cases. This underscores the significance of preoperative anticipation of tumour thrombus consistency, as these histological traits are intrinsic to its fragile variant.

Precise differentiation of VTT consistency is only sometimes possible using contemporary imaging modalities [18,19]. In general, CT and MRI demonstrate equal performance in detecting and defining the spread of IVC tumour thrombi in patients with RCC, with some advantages of the

Table 4
The diagnostic performance of mean ADC value, median, 10th percentile, entropy and skewness in differentiating between solid and friable tumour thrombus in patients with RCC.

Radiomic feature	Threshold value	Sensitivity	Specificity	AUC (95 % CI)	P value
Mean	1240.0 mm^2/s	0.93	0.69	0.857 (0.704–1.0)	0.002
Median	1249.0 mm^2/s	0.93	0.69	0.860 (0.709–1.0)	0.001
10th percentile	859.50 mm^2/s	0.86	0.62	0.734 (0.530–0.937)	0.039
Entropy	5.29	0.93	0.69	0.808 (0.633–0.983)	0.007
Skewness	0.09	0.86	0.92	0.931 (0.840–1.0)	<0.001

Abbreviations: AUC – area under the curve, CI – confidence interval.

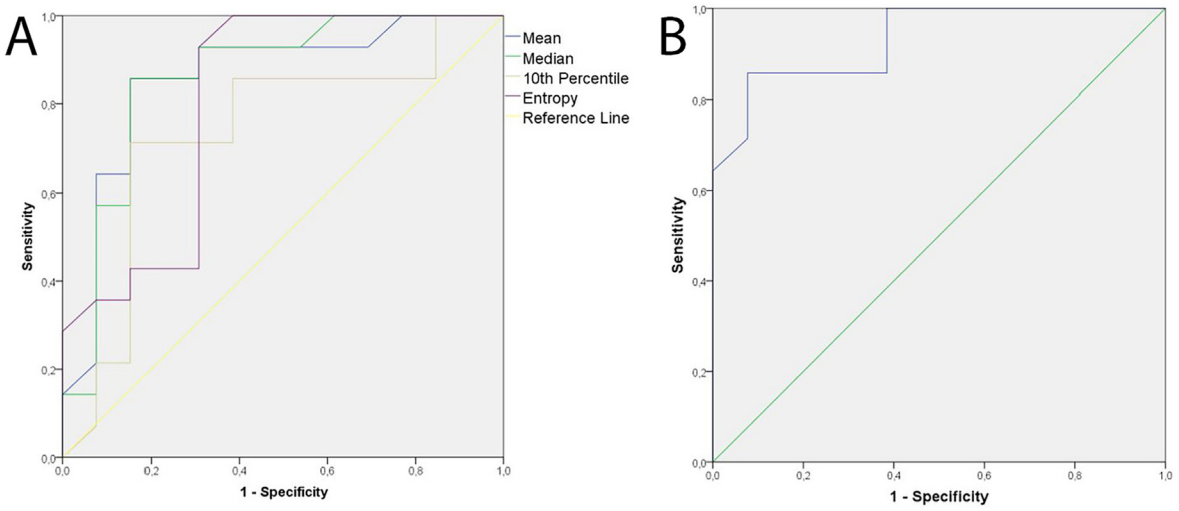

Fig. 5. Receiver operation characteristics (ROC) of mean ADC value, median, 10th percentile, entropy (A) and skewness (B) in differentiating between solid and friable tumour thrombus in patients with RCC.

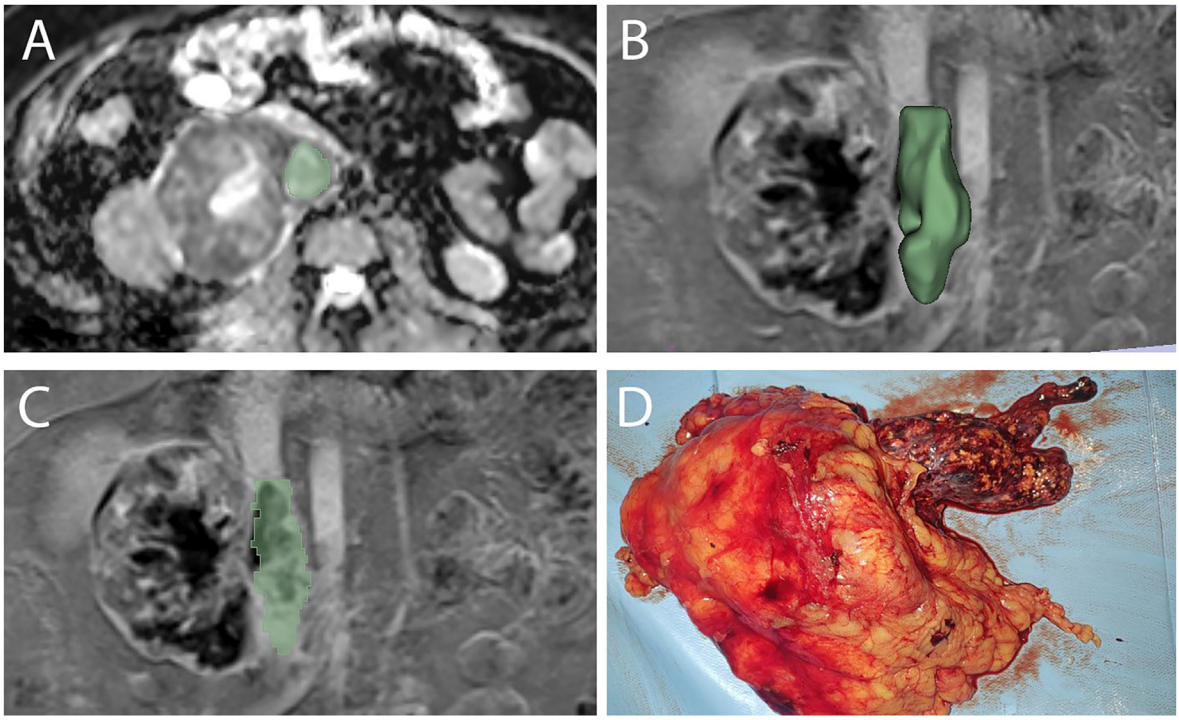

Fig. 6. Abdominal MRI of a 68 years old patient, with the right kidney conventional RCC and tumour thrombus in IVC, T3bN0M0, G3, histologically confirmed solid variant of thrombus (80 % of tumour cells). (A) ADC map with region of interest (ROI) over the region of the tumour thrombus in IVC; (B) 3D model of the tumour thrombus processed from the segmentation of ADC map, thrombus volume = 25 cm^3, 3D texture analysis revealed a solid thrombus; (C) coronal T2-WI with the corresponding ROI; (D) photography of kidney and tumour thrombus specimen after nephrectomy, intraoperative palpation was concordant with histological findings (solid thrombus).

latter [30,31]. While contrast-enhanced CT is used more often than MRI in this category of patients, the latter may offer some preponderances in the identification and characterization of IVC thrombi, such as the possibility of avoiding contrast usage, no radiation exposure of the patient and using flow-sensitive sequences [32,33]. Currently, there are no studies directly comparing the accuracy of CT and MRI in the differentiation of IVC thrombus consistency, nor standardized imaging techniques or definite imaging signatures for differentiation of IVC thrombus consistency. The role of DWI of MRI for this purpose is essential, yet remains unclear.

The data obtained in our earlier studies [34–36] demonstrated a significant restriction of hydrogen molecule diffusion in the tissues of conventional RCC compared to the healthy renal parenchyma, preconditioned by the greater density of the tumour. A statistically significant difference in mean ADC values of RCC with different grades of Fuhrman nuclear pleomorphism was observed - low-grade tumours showed higher mean ADC values compared to high-grade tumours. The MRI DWI modality and ADC measurement allowed for reliable differentiation between solid RCC of main histologic subtypes and grades, cystic RCC, benign renal lesions, and small renal masses. The data was

substantiated by recent meta-analyses, indicating that DWI exhibited the potential to differentiate between high-grade and low-grade clear cell RCC [37,38]. In another meta-analysis by Surov et al. [39] regarding the correlation between mean ADC value and RCC tumour cellularity, the authors showed an association between the investigated parameters ($p = -0.53$). Moreover, prior research has recognized a correlation between ADC and immunohistochemical markers of tumour proliferation, such as KI 67 in urinary tract cancers [40,41]. Our work was dedicated to assessing the efficiency of ADC of DWI-MRI in differentiating friable from solid IVC tumour thrombus in patients with RCC using 3D texture analysis.

To date, only a handful of scientific works elucidate the possibilities of contemporary imaging techniques such as CT, MRI or CEUS in differentiating tumour thrombi consistency, primarily in patients with RCC and HCC. Tublin et al. in their retrospective study ($n = 58$), found that in patients with cirrhosis, contrast-enhanced CT allowed for the identification of malignant venous thrombus using such imaging parameters as neovascularity or thrombus diameter greater than or equal to 23 mm with sensitivity and specificity of 86 % and 100 %, respectively [42]. Later, Canellas et al. [43], using contrast-enhanced CT texture analysis and thrombus density in patients with HCC and portal vein thrombosis ($n = 109$), found that in differentiating neoplastic from bland thrombus, the most discriminative parameters were entropy ($p < 0.001$), mean value of positive pixels ($p < 0.001$) and mean thrombus density ($p < 0.001$). The sensitivity and specificity were 95 % and 92 % for positive pixels, 87 % and 85 % for entropy, and 92 % and 85 % for mean thrombus density, respectively, with a combined AUC of 0.99 [43]. In our study, 3D texture analysis revealed that the radiomic features that demonstrated a significant difference between friable and solid thrombus consistency were mean ADC value, median, 10th percentile, entropy and skewness measured from ADC maps, with sensitivity and specificity for the skewness of 86 % and 92 %, respectively.

Contrast-enchanted MRI is a valuable tool for detecting and characterizing IVC thrombi. Earlier, it was demonstrated that preoperative magnetic resonance venography (1.0-T) allowed for more accurate differentiation of neoplastic from bland RCC venous involvement using FLASH-enhanced MR images (sensitivity 89 % and specificity 96 %) compared to signal intensity and pre-contract FLASH images (sensitivity 79 % and specificity 94 %), McNemar's test $p < 0.05$. Even though the radiological diagnosis was verified pathologically, one of the limitations of this study is the lack of clear pathomorphological criteria for solid and friable thrombi [44]. According to Akin et al. [32], friable thrombi were most commonly found in the liver (35 %) and retroperitoneal cancers (24 %) and most cases were located in the IVC (45 %) and the portal vein (22 %), while solid tumour thrombi were most commonly observed in RCC (55 %) and HCC (32 %). In contrast, the primary imaging feature able to differentiate solid from bland thrombus was the presence of contrast enhancement ($n = 171$). The significant limitation of this study was the lack of pathological verification of radiological diagnosis. In our present study, differentiation of friable from solid venous thrombi was possible in a pre-contrast setting, using the DWI sequence and ADC map calculated from it. This can be of high importance for the design of the surgical treatment in patients with contraindications to contrast media administration.

In their work, Catalano et al. [23] reported the feasibility of ADC of DWI MRI (1.5-T, *b*-values of 50, 400, and 800 s/mm^2) for differentiation of venous malignant thrombus from a friable one in HCC patients. The mean ADC of solid and friable (bland) venous thrombus were 0.88×10^{-3} mm^2/s and 2.89×10^{-3} mm^2/s, respectively. The ADC ratio of the thrombus to the tumour in the friable thrombus group was 2.9 compared to 0.998 in the solid thrombus consistency group ($P = 0.0003$) [23]. This work faced drastic criticism due to inconsistency with previous observations of other authors, namely, regarding the degree of diffusion restriction by hematomas - most of them tend to demonstrate low ADCs (contrary to Catalano et al. [23] findings), reflecting the restricted motion of water molecules due to the cellularity and viscosity of the fibrotic component [45]. In contrast to the previous study, Ahn et al. [24] suggested that the application of DWI MRI for differentiating benign from malignant portal vein thrombosis cannot differentiate the benign from malignant venous thrombi accurately due to considerable overlap of the ADC values, namely, the mean ADC of friable and solid portal venous thrombi were $1.0 \pm 0.39 \times 10^{-3}$ mm^2/s and $0.92 \pm 0.25 \times 10^{-3}$ mm^2/s, respectively ($p = 0.799$). In our study, in the MRI performed using a 1.5 T body scanner (*b*-values of 50, 200, 800 s/mm^2; Signa HDxt, General Electric), friable thrombi demonstrated significantly lower ADCs compared to solid ones: 1219.45 ± 114.88 vs 1454.16 ± 243.93 mm^2/s, respectively ($p = 0.002$). The mean 10th percentile of ADC value in friable compared to solid thrombi showed similar propensity ($p = 0.039$).

The role of ultrasound in differentiating friable from solid venous thrombi in patients with RCC is still undefined. In one recent study, using CEUS in patients with RCC complicated with IVC thrombus for differentiating its bland from solid consistency, the sensitivity, specificity accuracy, positive predictive value and negative predictive value were 100 %, 96 %, 96 %, 83 %, and 100 %, respectively, but only in an intraoperative setting [20]. In another later retrospective study, the sensitivity of CEUS used with the same purpose did not exceed 87.5 % [46].

4.1. Limitations of the study

The main limitations of our study are the relatively small cohorts of patients with solid and friable venous thrombi and the lack of comparison between MRI and CT imaging data, considering that CT remains the standard for visualizing this pathology.

5. Conclusions

In patients with RCC and tumour thrombus in the renal vein or IVC, the 3D texture analysis based on ADC map allows for precise differentiation of solid from a friable variant of the thrombus. This can be particularly important for surgical treatment planning and in patients with CT or contrast media contraindications.

Financial disclosure

The authors have no funding to disclose.

The author contribution

Study Design: Paweł Kowal, Peter Kruzliak, Yulian Mytsyk Data.

Collection: Paweł Kowal, Krzysztof Ratajczyk, Wiktor Bursiewicz, Maciej Trzciniecki, Karolina Marek-Bukowiec, Joanna Rogala, Vasyl Kowalskyi.

Statistical Analysis: Joanna Rogala, Vasyl Kowalskyi, Jozef Dragasek.

Data Interpretation: Paweł Kowal, Krzysztof Ratajczyk, Wiktor Bursiewicz, Maciej Trzciniecki, Andrea Botikova, Peter Kruzliak, Yulian Mytsyk.

Manuscript Preparation: Paweł Kowal, Krzysztof Ratajczyk, Wiktor Bursiewicz, Maciej Trzciniecki, Peter Kruzliak, Yulian Mytsyk Literature Search: Karolina Marek-Bukowiec, Joanna Rogala, Vasyl Kowalskyi, Andrea Botikova.

Funds Collection: n/a.

Funds collection

N/a.

Data statement/availability of data and material

The authors declare that there are no datasets or materials associated with this study available for sharing.

Declaration of generative AI and AI-assisted technologies in the writing process

During the preparation of this work the authors did not use any AI-assisted technology.

Declaration of competing interest

The authors declare that they have no known competing financial interests or personal relationships that could have appeared to influence the work reported in this paper.

References

[1] Bukavina L, Bensalah K, Bray F, Carlo M, Challacombe B, Karam JA, Kassouf W, Mitchell T, Montironi R, O'Brien T, Panebianco V, Scelo G, Shuch B, van Poppel H, Blosser CD, Psutka SP. Epidemiology of renal cell carcinoma: 2022 update. Eur Urol 2022 Nov;82(5):529–42. https://doi.org/10.1016/j.eururo.2022.08.019. Epub 2022 Sep. 10.

[2] Boussios S, Devo P, Goodall ICA, Sirlantzis K, Ghose A, Shinde SD, et al. Exosomes in the diagnosis and treatment of renal cell cancer. Int J Mol Sci 2023;24:14356.

[3] Mytsyk Y, Dosenko V, Borys Y, Kucher A, Gazdikova K, Busselberg D, et al. MicroRNA-15a expression measured in urine samples as a potential biomarker of renal cell carcinoma. Int Urol Nephrol 2018;50:851–9.

[4] Tordjman M, Mali R, Madelin G, Prabhu V, Kang SK. Diagnostic test accuracy of ADC values for identification of clear cell renal cell carcinoma: systematic review and meta-analysis. Eur Radiol 2020;30:4023–38. https://doi.org/10.1007/s00330-020-06740-w.

[5] SEER*Explorer. An interactive website for SEER cancer statistics [Internet]. In: Surveillance research program. National Cancer Institute; 2024 Apr 17 [updated: 2024 Jun 27; cited 2024 Sep 9]. Available from: https://seer.cancer.gov/statistics-network/explorer/.

[6] Rassy E, Parent P, Lefort F, Boussios S, Baciarello G, Pavlidis N. New rising entities in cancer of unknown primary: is there a real therapeutic benefit? Crit Rev Oncol Hematol 2020;147:102882.

[7] Hevia V, Ciancio G, Gómez V, Álvarez S, Díez-Nicolás V, Burgos FJ. Surgical technique for the treatment of renal cell carcinoma with inferior vena cava tumor thrombus: tips, tricks and oncological results. SpringerPlus 2016;5:132.

[8] Moinzadeh A, Libertino JA. Prognostic significance of tumor thrombus level in patients with renal cell carcinoma and venous tumor thrombus extension. Is all T3b the same? J Urol 2004;171:598–601.

[9] Haferkamp A, Bastian PJ, Jakobi H, Pritsch M, Pfitzenmaier J, Albers P, et al. Renal cell carcinoma with tumor thrombus extension into the vena cava: prospective long-term followup. J Urol 2007;177(5):1703–8.

[10] Ljungberg B, Albiges L, Abu-Ghanem Y, Bedke J, Capitanio U, Dabestani S, et al. European association of Urology guidelines on renal cell carcinoma: the 2022 update. Eur Urol 2022;82(4):399–410.

[11] Baheen Q, Liu Z, Hao Y, Sawh RRR, Li Y, Zhao X, et al. The significant role of tumor volume on the surgical approach choice, surgical complexity, and postoperative complications in renal cell carcinoma with venous tumor thrombus from a large Chinese center experience. Front Oncol 2022;12:869891.

[12] Ayyathurai R, Garcia-Roig M, Gorin MA, González J, Manoharan M, Kava BR, et al. Bland thrombus association with tumour thrombus in renal cell carcinoma: analysis of surgical significance and role of inferior vena caval interruption. BJU Int 2012;110(11 Pt B):E449–55.

[13] Hutchinson R, Rew C, Chen G, Woldu S, Krabbe LM, Meissner M, et al. The adverse survival implications of bland thrombus in renal cell carcinoma with venous tumor thrombus. Urology 2018;115:119–24.

[14] Liu Z, Zhang L, Hong P, Li L, Tang S, Zhao X, et al. The influence of venous tumor thrombus combined with bland thrombus on the surgical treatment and prognosis of renal cell carcinoma patients. Cancer Med 2020;9(16):5860–8.

[15] Zhuo L, Zhang L, Li L, Zhang H, Tang S, Zhao X, et al. Mp57-06 bland thrombus as an independent risk factor for survival implications in renal cell carcinoma with venous tumor thrombus. J Urol 2020;203(Supplement 4):e859–61.

[16] Blute ML, Leibovich BC, Lohse CM, Cheville JC, Zincke H. The Mayo Clinic experience with surgical management, complications and outcome for patients with renal cell carcinoma and venous tumour thrombus. BJU Int 2004;94(1):33–41.

[17] Chen K, Liu Z, Li Y, Zhao X, Zhang S, Liu C, et al. Diagnosis and treatment strategies for intraoperative pulmonary embolism caused by renal tumor thrombus shedding. J Card Surg 2022;37(11):3973–83.

[18] Rohatgi S, Howard SA, Tirumani SH, Ramaiya NH, Krajewski KM. Multimodality imaging of tumour thrombus. Can Assoc Radiol J 2015;66(2):121–9.

[19] Tabbara MM, Farag A, Ciancio G. Renal cell carcinoma with inferior vena cava tumor thrombus initially misdiagnosed as bland thrombus due to hypercoagulable state, vol. 10. SAGE Open Med Case Rep; 2022. p. 2050313X221102019.

[20] Li QY, Li N, Huang QB, Luo YK, Wang BJ, Guo AT, et al. Contrast-enhanced ultrasound in detecting wall invasion and differentiating bland from tumor thrombus during robot-assisted inferior vena cava thrombectomy for renal cell carcinoma. Cancer Imag 2019;19(1):79.

[21] Zhang L, Yang G, Shen W, Qi J. Spectrum of the inferior vena cava: MDCT findings. Abdom Imag 2007;32(4):495–503.

[22] Wang K, Liu Z, Hong P, Qin YC, Zhao X, Zhang HX, et al. T.H.R.O.B.V.S. Score - a comprehensive model to predict the surgical complexity of renal cell carcinoma with tumor thrombus. Front Oncol 2022;12:900550.

[23] Catalano OA, Choy G, Zhu A, Hahn PF, Sahani DV. Differentiation of malignant thrombus from bland thrombus of the portal vein in patients with hepatocellular carcinoma: application of diffusion-weighted MR imaging. Radiology 2010;254(1):154–62.

[24] Ahn JH, Yu JS, Cho ES, Chung JJ, Kim JH, Kim KW. Diffusion-weighted MRI of malignant versus benign portal vein thrombosis. Korean J Radiol 2016;17(4):533–40.

[25] Qin Z, Li R, Qin Y. Prognostic significance of venous tumor thrombus consistency (solid vs. friable) in patients with renal cell carcinoma: a systematic review and meta-analysis. AME Medical Journal [Internet] 2018 Jun 14;3(0) [cited 2020 Jan 18], http://amj.amegroups.com/article/view/4509.

[26] Oto A, Herts BR, Remer EM, Novick AC. Inferior vena cava tumor thrombus in renal cell carcinoma: staging by MR imaging and impact on surgical treatment. AJR Am J Roentgenol 1998;171(6):1619–24.

[27] Bertini R, Roscigno M, Freschi M, Strada E, Angiolilli D, Petralia G, et al. Impact of venous tumour thrombus consistency (solid vs friable) on cancer-specific survival in patients with renal cell carcinoma. Eur Urol 2011;60:358–65.

[28] Wang H, Li X, Huang Q, Panic A, Shen D, Jia W, et al. Prognostic role of bland thrombus in patients treated with resection of renal cell carcinoma with inferior vena cava tumor thrombus. Urol Oncol 2021;39:302.e1–7. https://doi.org/10.1016/j.urolonc.2021.02.005.

[29] Weiss VL, Braun M, Perner S, Harz A, Vorreuther R, Kristiansen G, et al. Prognostic significance of venous tumour thrombus consistency in patients with renal cell carcinoma (RCC). BJU Int 2014;113:209–17. https://doi.org/10.1111/bju.12322.

[30] Cuevas C, Raske M, Bush WH, Takayama T, Maki JH, Kolokythas O, et al. Imaging primary and secondary tumor thrombus of the inferior vena cava: multi-detector computed tomography and magnetic resonance imaging. Curr Probl Diagn Radiol 2006;35(3):90–101.

[31] Lawrentschuk N, Gani J, Riordan R, Esler S, Bolton DM. Multidetector computed tomography vs magnetic resonance imaging for defining the upper limit of tumour thrombus in renal cell carcinoma: a study and review. BJU Int 2005;96(3):291–5.

[32] Akin O, Dixit D, Schwartz L. Bland and tumor thrombi in abdominal malignancies: magnetic resonance imaging assessment in a large oncologic patient population. Abdom Imag 2011;36(1):62–8.

[33] Zhang LJ, Wu X, Yang GF, Tang CX, Luo S, Zhou CS, et al. Three-dimensional contrast-enhanced magnetic resonance venography for detection of renal vein thrombosis: comparison with multidetector CT venography. Acta Radiol 2013;54(10):1125–31.

[34] Mytsyk Y, Dutka I, Borys Y, Komnatska I, Shatynska-Mytsyk I, Farooqi AA, et al. Renal cell carcinoma: applicability of the apparent coefficient of the diffusion-weighted estimated by MRI for improving their differential diagnosis, histologic subtyping, and differentiation grade. Int Urol Nephrol 2017;49(2):215–24.

[35] Mytsyk Y, Borys Y, Komnatska I, Dutka I, Shatynska-Mytsyk I. Value of the diffusion-weighted MRI in the differential diagnostics of malignant and benign kidney neoplasms - our clinical experience. Pol J Radiol 2014;79:290–5.

[36] Mytsyk Y, Dutka I, Yuriy B, Maksymovych I, Caprnda M, Gazdikova K, et al. Differential diagnosis of the small renal masses: role of the apparent diffusion coefficient of the diffusion-weighted MRI. Int Urol Nephrol 2018;50(2):197–204.

[37] Woo S, Suh CH, Kim SY, Cho JY, Kim SH. Diagnostic performance of DWI for differentiating high- from low-grade clear cell renal cell carcinoma: a systematic review and meta-analysis. AJR Am J Roentgenol 2017;209(6):W374–81.

[38] Tordjman M, Mali R, Madelin G, Prabhu V, Kang SK. Diagnostic test accuracy of ADC values for identification of clear cell renal cell carcinoma: systematic review and meta-analysis. Eur Radiol 2020;30(7):4023–38.

[39] Surov A, Meyer HJ, Wienke A. Correlation between apparent diffusion coefficient (ADC) and cellularity is different in several tumors: a meta-analysis. Oncotarget 2017;8(35):59492–9.

[40] Sevcenco S, Haitel A, Ponhold L, Susani M, Fajkovic H, Shariat SF, et al. Quantitative apparent diffusion coefficient measurements obtained by 3-Tesla MRI are correlated with biomarkers of bladder cancer proliferative activity. PLoS One 2014;9(9):e106866.

[41] Yoshida S, Kobayashi S, Koga F, Ishioka J, Ishii C, Tanaka H, et al. Apparent diffusion coefficient as a prognostic biomarker of upper urinary tract cancer: a preliminary report. Eur Radiol 2013;23(8):2206–14.

[42] Tublin ME, Dodd GD, Baron RL. Benign and malignant portal vein thrombosis: differentiation by CT characteristics. AJR Am J Roentgenol 1997;168:719–23.

[43] Canellas R, Mehrkhani F, Patino M, Kambadakone A, Sahani D. Characterization of portal vein thrombosis (neoplastic versus bland) on CT images using software-based texture analysis and thrombus density (hounsfield units). AJR Am J Roentgenol 2016;207:W81–7.

[44] Laissy JP, Menegazzo D, Debray MP, Toublanc M, Ravery V, Dumont E, et al. Renal carcinoma: diagnosis of venous invasion with Gd-enhanced MR venography. Eur Radiol 2000;10(7):1138–43.

[45] Yu JS, Chung JJ, Kim JH, Kim KW. Limited value of diffusion-weighted MR imaging for differentiating bland from malignant portal venous thrombi. Radiology 2010;256(2):673–4. author reply 674.

[46] Li Q, Wang Z, Ma X, Tang J, Luo Y. Diagnostic accuracy of contrast-enhanced ultrasound for detecting bland thrombus from inferior vena cava tumor thrombus in patients with renal cell carcinoma. Int Braz J Urol 2020;46(1):92–100.